

Higgs-mass dependence of the effective electroweak mixing angle $\sin^2 \theta_e$ at the two-loop level

W. Hollik, U. Meier and S. Uccirati

Max-Planck-Institut für Physik
(Werner-Heisenberg-Institut)
D-80805 München, Germany

Abstract

The result for the Higgs-dependent electroweak two-loop bosonic contributions to the effective leptonic mixing angle of the Z-boson in the Standard Model is presented. Together with the previously calculated fermionic contributions it yields the complete dependence of $\sin^2 \theta_e$ on the Higgs-boson mass M_H at the two-loop level. Compared to the fermionic contributions, the bosonic contributions are found to be smaller, but large enough to induce a non-negligible modification of the M_H dependence.

1 Introduction

The effective electroweak mixing angle for leptons, $\sin^2 \theta_e$, is experimentally determined with high accuracy from measurements of various asymmetries on the Z resonance, with the current value 0.23153 ± 0.00016 [1], and further improvements are expected from future collider experiments [2, 3]. Analyses done in combination with the theoretical predictions for $\sin^2 \theta_e$ in the Standard Model yield stringent bounds on the Higgs-boson mass M_H , making $\sin^2 \theta_e$ a precision observable of central importance for tests of the Standard Model. Therefore, a precise and reliable calculation is a necessity, requiring at least the complete electroweak two-loop contributions.

$\sin^2 \theta_e$ is determined from the ratio of the dressed vector and axial vector couplings $g_{V,A}$ of the Z boson to leptons [4],

$$\sin^2 \theta_e = \frac{1}{4} \left(1 - \text{Re} \frac{g_V}{g_A} \right) : \quad (1)$$

It is related to the vector boson-mass ratio or the on-shell quantity s_W^2 , respectively, via

$$\sin^2 \theta_e = s_W^2 = 1 - \frac{M_W^2}{M_Z^2} ; \quad c_W^2 = 1 + \frac{M_W^2}{M_Z^2} ; \quad (2)$$

involving the c_W factor, which is unity at the tree level and accommodates the higher-order contributions in α . In recent independent calculations the complete two-loop electroweak corrections of the fermionic type, i.e. with at least one closed fermion loop, to $\sin^2 \theta_e$ were obtained [5, 6]. The bosonic two-loop corrections, however, are still missing. In this note we present a first step towards the full $\mathcal{O}(\alpha^2)$ result for $\sin^2 \theta_e$, namely the results of the subclass of Higgs dependent contributions, thus providing the complete Higgs-boson mass dependence of the bosonic two-loop corrections.

2 Structure of electroweak two-loop contributions

The general strategy of our calculation of the two-loop electroweak contributions to $\sin^2 \theta_e$, including renormalization, has been described in [6]. As outlined in [6], one has to take into account basically the classes of diagrams depicted schematically in Fig. 1, where the circles denote renormalized two- and three-point irreducible vertex functions at the one-loop level in Fig. 1a and at two-loop order in Fig. 1c and 1d.

The real part of the diagram shown in Fig. 1c vanishes in the on-shell renormalization scheme [7] adopted in our calculation and the diagrams of Fig. 1a and 1b only contribute products of imaginary parts of one-loop functions. So we are left with the irreducible two-loop Z $\gamma\gamma$ -vertex diagrams in Fig. 1d. The Z couplings in (1) appear in the renormalized Z $\gamma\gamma$ -vertex for on-shell Z bosons,

$$\hat{\Gamma}_Z^{\gamma\gamma(2)}(M_Z^2) = (g_V - g_A \gamma_5) : \quad (3)$$

As for the fermionic corrections, we split the two-loop contribution for the renormalized vertex into two UV-finite pieces according to

$$\begin{aligned}\hat{\Gamma}_Z^{(2)}(P^2) &= \Gamma_Z^{(2)}(M_Z^2) + \text{CT} \\ &= \Gamma_Z^{(2)}(0) + \text{CT} + \left[\Gamma_Z^{(2)}(M_Z^2) - \Gamma_Z^{(2)}(0) \right] : \quad (4)\end{aligned}$$

$\Gamma_Z^{(2)}(P^2)$ denotes the corresponding unrenormalized Z vertex for on-shell leptons and momentum transfer P^2 , and CT is the two-loop counter term, which is independent of P^2 . The first term in the decomposition of (4) therefore contains the complete two-loop renormalization, but no genuine two-loop vertex diagrams since in absence of external momenta they reduce to simpler vacuum integrals. All the genuine two-loop vertex diagrams appear as subtracted quantities in the second term in (4).

As a first step towards the complete bosonic two-loop corrections, we consider the

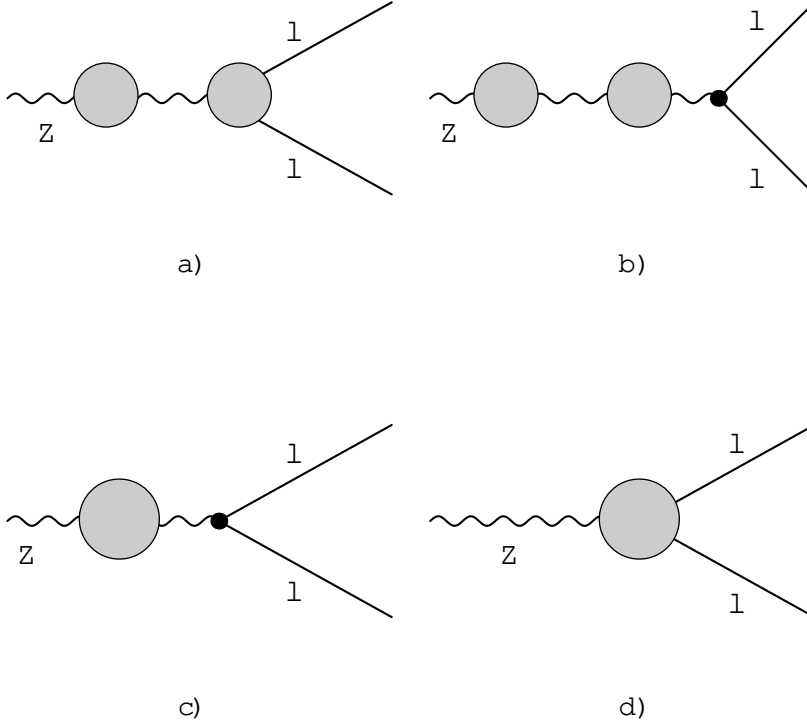


Figure 1: Generic classes of two loop diagrams

Higgs-mass dependence. To this end we calculate the subtracted two-loop bosonic

$$\binom{2}{\text{bos;sub}} = \binom{2}{\text{bos}} (\mathbb{M}_H) \binom{2}{\text{bos}} \mathbb{M}_H^0; \quad (5)$$

for a fixed reference mass of the Higgs boson, chosen as $M_H^0 = 100 \text{ GeV}$. The quantity $\Gamma_{\text{bos;sub}}^{(2)}$ is UV finite and gauge-parameter independent. The dependence on M_H enters exclusively through diagrams with internal Higgs boson lines. Some typical examples are displayed in Fig. 2.

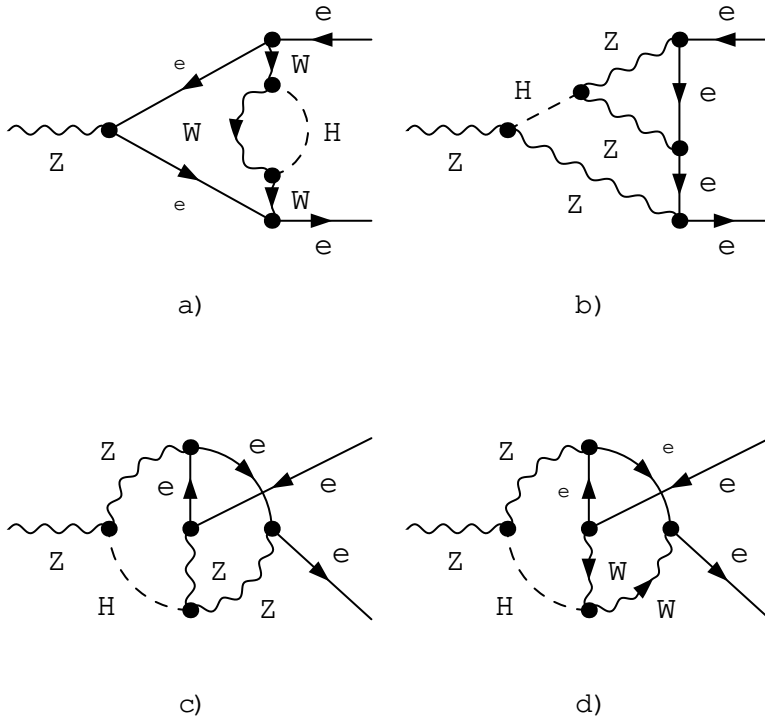


Figure 2: Examples of diagrams containing internal Higgs bosons

The computation of the renormalized vertex at $P^2 = 0$ [rst term in (4)] can be done in analogy to the fermionic case [6], which means generating Feynman diagrams with FeynArts [8] and applying TwoCalc [9] to reduce the amplitudes to standard integrals. The resulting scalar one-loop integrals and two-loop vacuum integrals are calculated using known analytic results [10, 11]. The two-loop self-energies with non-vanishing external momentum, as part of the two-loop counterterm, are obtained with the help of one-dimensional integral representations [12]. Moreover, we implemented new methods described in [13], and used them for cross checks.

For the subtracted vertex, the second term in equation (4), two independent calculations were performed, based either on FeynArts or on GraphShot [14] for generating the vertex amplitudes. The diagrams containing self-energy subloops (e.g. Fig. 2a) were evaluated using the method of one-dimensional integral representations, as described in [6]. In addition, as an independent check, the methods described in [13] were implemented and applied. The diagrams containing vertex subloops (e.g. Fig. 2b) were also calculated as in the fermionic case, using the methods described in [13]. The only new type of diagrams compared to the fermionic case are the two non-planar diagrams in Fig. 2c,d. The method used for their evaluation is explained in the next section.

3 Non-planar diagrams

The non-planar diagrams in Fig. 2c,d are UV-finite and can be evaluated in 4 dimensions. We have to deal with diagrams of the type

$$V_{222}^{(i)} = \int_0^1 \int_0^1 d^4 q_1 d^4 q_2 \frac{(q_1; q_1 q_2)}{[1][2][3][4][5][6]}, \quad (6)$$

with the following short-hand notation for the propagators,

$$\begin{aligned} [1] &= q_1^2 - M_V^2; & [2] &= (q_1 - p_1)^2; & [3] &= (q_1 - q_2 + p_1)^2 - M_H^2; \\ [4] &= (q_1 - q_2 - p_2)^2 - M_Z^2; & [5] &= q_2^2; & [6] &= (q_2 - p_1)^2 - M_V^2; \\ M_V &= (M_W; M_Z): \end{aligned} \quad (7)$$

Following the discussion given in [13], we first combine the propagators [1] and [2] with a Feynman-parameter z_1 , the propagators [3] and [4] with a Feynman-parameter z_2 and the propagators [5] and [6] with a Feynman-parameter z_3 . Then we change variables according to $q_1 \rightarrow q_1 + z_1 p_2$, $q_2 \rightarrow q_2 + z_3 p_1$ and combine the q_1 and $q_1 - q_2$ propagators with a parameter x . After the q_1 -integration we combine the residual propagators with a parameter y and carry out the q_2 integration.

Since we consider the external fermions to be massless we have $p_{1,2}^2 = 0$. In this situation, the expression for V_{222} is much simpler than in the general case because we have just to deal with integrals of the type

$$\int_0^1 \int_0^1 dx dy dz_1 dz_2 dz_3 z_3^n (a z_1 z_3 + b z_3 + c z_1 + d)^{-2} \quad (8)$$

with $n = 0; 1; 2$. a, b, c, d are functions of the internal masses, of the external Z momentum and of the parameters x, y, z_2 , but they are independent of z_1 and z_3 . For $n = 0$ we perform the integrations in z_1 and z_3 analytically,

$$\int_0^1 \int_0^1 dz_1 dz_3 (a z_1 z_3 + b z_3 + c z_1 + d)^{-2} = \frac{1}{ad - bc} \ln \left| 1 + \frac{ad - bc}{(c + d)(b + d)} \right|; \quad (9)$$

whereas for $n = 1; 2$ the z_1 integration and an integration by parts in z_3 are done analytically,

$$\int_0^1 \int_0^1 dz_1 dz_3 z_3^n (a z_1 z_3 + b z_3 + c z_1 + d)^{-2} = \int_0^1 dz_3 \frac{z_3^{n-1}}{ad - bc} \ln \left(1 + \frac{(1 - z_3)(ad - bc)}{((a + b)z_3 + c + d)(b + d)} \right) : \quad (10)$$

In both cases smooth integrands are obtained, suitable for follow-up numerical integrations. The algebraic handling and the numerical evaluation were performed in two independent computations for cross-checking the results. For the numerical integration the NAG library D01GDF [15] was used in one case and the CUBA library [16] in the other case.

4 Results

The evaluation and presentation of the final result are done for the set of input parameters put together in Tab. 1. M_W and M_Z are the experimental values of the W^- and Z^- boson masses [17], which are the on-shell masses. They have to be converted to the values in the pole mass scheme [7], labeled as \overline{M}_W and \overline{M}_Z , which are used internally for the calculation. These quantities are related via $M_{W,Z} = \overline{M}_{W,Z} + \frac{\delta}{M_{W,Z}} = (2 M_{W,Z})$. For \overline{M}_Z the experimental value (Tab. 1) and for \overline{M}_W the theoretical value has been used, i.e. $\overline{M}_W = 3 G M_W^3 = 2 \sqrt{2} (1 + 2 s(M_W^2)) = (3 \text{ GeV})$ with sufficient accuracy.

parameter	value
M_W	80.426 GeV
M_Z	91.1876 GeV
m_t	178.0 GeV
(M_Z^2)	0.05907
$s(M_Z^2)$	0.117
G	$1.16637 \cdot 10^{-5}$
\overline{M}_W	80.3986 GeV
\overline{M}_Z	91.1535 GeV

Table 1: Input parameters entering our computation. M_W and M_Z are the experimental values of the W^- and Z^- boson masses, whereas \overline{M}_W and \overline{M}_Z are the calculated quantities in the pole mass scheme.

The results are given for α_s , eq. (2), and are listed in Tab. 2 for different values of M_H . For comparison, Tab. 2 also contains the values of the fermionic corrections and the corresponding subtracted quantity $\delta_{\text{ferm;sub}}^{(2)} = \delta_{\text{ferm}}^{(2)}(M_H) - \delta_{\text{ferm}}^{(2)}(M_H^0)$.

In the considered range of the Higgs-boson mass, the bosonic result has the opposite sign and is not dramatically smaller than the fermionic contribution and thus changes

M_H [GeV]	$(^{(2)})_{\text{ferm}} \cdot 10^{-4}$	$(^{(2)})_{\text{ferm;sub}} \cdot 10^{-4}$	$(^{(2)})_{\text{bos;sub}} \cdot 10^{-4}$
100	-0.637 (1)	0	0
200	-2.165 (1)	-1.528	0.265
600	-5.012 (1)	-4.375	0.914
1000	-4.737 (1)	-4.100	1.849

Table 2: Two-loop result for $\sin^2 \theta_e$ in comparison with the fermionic contributions

the Higgs-mass dependence of the electroweak 2-loop corrections to $\sin^2 \theta_e$ significantly. The uncertainties from numerical integration in the bosonic result are of the order 10^{-9} and hence negligible.

In conclusion, we have evaluated the bosonic electroweak 2-loop corrections to $\sin^2 \theta_e$ containing internal Higgs bosons. As a new feature, non-planar vertex diagrams appear, and a method to calculate such non-planar diagrams has been described. Our numerical result for $(^{(2)})$ shows that the Higgs-mass dependence of the two-loop prediction for $\sin^2 \theta_e$ is affected sizeably by the bosonic contributions.

S.J. would like to express his gratitude to Stefano Actis for making available the beta version of GraphShot, a FORM code for generating and reducing standard model one- and two-loop diagrams which is presently under development at Torino University.

References

- [1] The LEP Collaborations, the LEP Electroweak Working Group, the SLD Electroweak and Heavy Flavour Groups, [arXiv:hep-ex/0509008](#).
- [2] J. A. Aguilar-Saavedra et al., TESLA Technical Design Report Part III: Physics at an e^+e^- Linear Collider [[hep-ph/0106315](#)]. T. Abe et al. [American Linear Collider Working Group Collaboration], in Proc. of the APS/DPF/DPB Summer Study on the Future of Particle Physics (Snowmass 2001) ed. R. Davidson and C. Quigg, SLAC-R-570, Resource book for Snowmass 2001 [[hep-ex/0106055](#), [hep-ex/0106056](#), [hep-ex/0106057](#), [hep-ex/0106058](#)]. K. Abe et al. [ACFA Linear Collider Working Group Collaboration], ACFA Linear Collider Working Group report, [[hep-ph/0109166](#)].
- [3] U. Baur, R. Clare, J. Erler, S. Heinemeyer, D. Wackeroth, G. Weiglein and D. R. Wood, in Proc. of the APS/DPF/DPB Summer Study on the Future of Particle Physics (Snowmass 2001) ed. N. Graf, [eConf C010630 \(2001\) P122](#) [[arXiv:hep-ph/0111314](#)].

- [4] D . Y . Bardin et al., hep-ph/9709229, in Precision Calculations for the Z Resonance, D . Bardin, W . Hollik, G . Passarino (Eds.), CERN 95-03.
- [5] M . Awramik, M . Czakon, A . Freitas and G . Weiglein, Phys. Rev. Lett. 93 (2004) 201805 [arXiv:hep-ph/0407317], Nucl. Phys. Proc. Suppl. 135 (2004) 119 [arXiv:hep-ph/0408207].
- [6] W . Hollik, U . Mier and S . Uccirati, arXiv:hep-ph/0507158.
- [7] A . Freitas, W . Hollik, W . Walter and G . Weiglein, Phys. Lett. B 495 (2000) 338, E : ibid. B 570 (2003) 260 [hep-ph/0007091] and Nucl. Phys. B 632 (2002) 189, E : ibid. B 666 (2003) 305 [hep-ph/0202131].
- [8] J . Kublbeck, M . Bohm and A . Denner, Comp. Phys. Comm. 60 (1990) 165. T . Hahn, Nucl. Phys. Proc. Suppl. 89 (2000) 231 [arXiv:hep-ph/0005029], Comput. Phys. Comm. 140 (2001) 418 [arXiv:hep-ph/0012260], FeynArts User's Guide , available at <http://www.feynarts.de>.
- [9] G . Weiglein, R . Scharf and M . Bohm , Nucl. Phys. B 416 (1994) 606 [arXiv:hep-ph/9310358]; G . Weiglein, R . Mertig, R . Scharf and M . Bohm , PRINT-95-128 Prepared for 2nd International Workshop on Software Engineering, Artificial Intelligence and Expert Systems for High-energy and Nuclear Physics, La Londe Les Maures, France, 13-18 Jan 1992
- [10] G . 't Hooft and M . J . G . Veltman, Nucl. Phys. B 153 (1979) 365.
- [11] A . I . Davydychev and J . B . Tausk, Nucl. Phys. B 397 (1993) 123.
- [12] S . Bauberger, M . Bohm , G . Weiglein, F . A . Berends and M . Buza, Nucl. Phys. Proc. Suppl. 37B (1994) 95 [arXiv:hep-ph/9406404]; S . Bauberger, F . A . Berends, M . Bohm and M . Buza, Nucl. Phys. B 434 (1995) 383 [arXiv:hep-ph/9409388]; S . Bauberger and M . Bohm , Nucl. Phys. B 445 (1995) 25 [arXiv:hep-ph/9501201].
- [13] A . Ferroglia, M . Passera, G . Passarino and S . Uccirati, Nucl. Phys. B 680 (2004) 199 [arXiv:hep-ph/0311186]; S . Actis, A . Ferroglia, G . Passarino, M . Passera and S . Uccirati, Nucl. Phys. B 703 (2004) 3 [arXiv:hep-ph/0402132]. G . Passarino, Nucl. Phys. B 619 (2001) 257 [arXiv:hep-ph/0108252]. G . Passarino and S . Uccirati, Nucl. Phys. B 629 (2002) 97 [arXiv:hep-ph/0112004].
- [14] S . Actis, A . Ferroglia, G . Passarino and M . Passera, GraphShot, a FORM package for generating, reducing and evaluating one and two loop Feynman diagrams (in preparation).
- [15] NAG Fortran Library, Mark 19, The Numerical Algorithms Group Ltd, Oxford UK . 1999.
- [16] T . Hahn, arXiv:hep-ph/0404043.

[17] S. Eidelman et al. [Particle Data Group], Phys. Lett. B 592 (2004) 1.